

A dynein independent role of Tctex-1 at the kinetochore

Chenshu Liu¹, Jen-Zen Chuang², Ching-Hwa Sung², and Yinghui Mao^{1,*}

¹Department of Pathology and Cell Biology; Columbia University College of Physicians and Surgeons; New York, NY USA; ²Department of Cell and Developmental Biology; Weill Medical College of Cornell University; New York, NY USA

Keywords: Tctex-1, dynein, mitosis, kinetochore

Dynein light chains are accessory subunits of the cytoplasmic dynein complex, a minus-end directed microtubule motor. Here, we demonstrate that the dynein light chain Tctex-1 associates with unattached kinetochores and is essential for accurate chromosome segregation. Tctex-1 knockdown in cells does not affect the localization and function of dynein at the kinetochore, but produces a prolonged mitotic arrest with a few misaligned chromosomes, which are subsequently missegregated during anaphase. This function is independent of Tctex-1's association with dynein. The kinetochore localization of Tctex-1 is independent of the ZW10-dynein pathway, but requires the Ndc80 complex. Thus, our findings reveal a dynein independent role of Tctex-1 at the kinetochore to enhance the stability of kinetochore-microtubule attachment.

Introduction

Accurate chromosome segregation during mitosis requires proper interactions between chromosomes and plus ends of microtubules of the mitotic spindle.^{1,2} The kinetochore, the proteinaceous complex assembled at the centromere region, serves as the microtubule attachment site at each mitotic chromosome.^{3,4} Although there is much support for the KMN network (KNL1, Mis12, and Ndc80 complexes) serving as the core microtubule binding apparatus at the kinetochore,^{5,6} it is quite clear that many other kinetochore- and microtubule-associated proteins play important roles in maintaining the stable connection between kinetochores and dynamic microtubule plus ends. Depletion of the Ska1/RAMA complex⁷⁻¹⁰ or a formin mDia3^{11,12} results in chromosome misalignment phenotypes in mammalian cultured cells, reminiscent of depletion of the Ndc80 complex. Two force-producing kinetochore-associated motors, the plus end-directed microtubule motor CENP-E and the minus end-directed microtubule motor cytoplasmic dynein, are associated with the outermost region of the kinetochore and have been implicated in the initial stages of microtubule interactions.¹³ A group of microtubule plus-end-tracking proteins are delivered to the kinetochore by microtubule plus ends and possibly act as tethers, as well as modulators of microtubule dynamics, at attachment sites.^{14,15}

The dynein light chains are accessory subunits of the cytoplasmic dynein motor complexes and form a complex with the

dynein intermediate chains at the base of the dynein heavy chains.¹⁶ While the light chains directly link dynein to its cargo as an adaptor protein,¹⁷ recent studies suggest that these noncatalytic subunits may play a dynein-independent role in diverse cellular functions. For example, the LC8 family members of dynein light chains have been shown to interact, besides dynein, with a large number of proteins.¹⁸ Similarly, the Tctex family member of Tctex-1 (or DYNLT1) has dynein-independent roles in actin remodeling during neurite outgrowth¹⁹ and in ciliary resorption.^{20,21} We now show that Tctex-1 associates with unattached kinetochores and participates in stable microtubule attachment independent of cytoplasmic dynein.

Results

Both Tctex-1 and CLIP-170 associate with dyneinless kinetochores

We have shown that the formin mDia3 and its interaction with EB1, a microtubule plus-end-tracking protein, are essential for accurate chromosome segregation.¹¹ Knockdown the mDia3 protein in cells results in a loss of EB1, but an increase of CLIP-170, another microtubule plus-end-tracking protein, at kinetochores aligned at the metaphase plate (Fig. 1A, B and D), judging by their relative signals against anti-centromere antibody (ACA) as the kinetochore marker. The compositional change of microtubule plus ends attached to kinetochores does

© Chenshu Liu, Jen-Zen Chuang, Ching-Hwa Sung, and Yinghui Mao

*Correspondence to: Yinghui Mao; Email: ym2183@columbia.edu

Submitted: 10/21/2014; Accepted: 12/15/2014

<http://dx.doi.org/10.1080/15384101.2014.1000217>

This is an Open Access article distributed under the terms of the Creative Commons Attribution-Non-Commercial License (<http://creativecommons.org/licenses/by-nc/3.0/>), which permits unrestricted non-commercial use, distribution, and reproduction in any medium, provided the original work is properly cited. The moral rights of the named author(s) have been asserted.

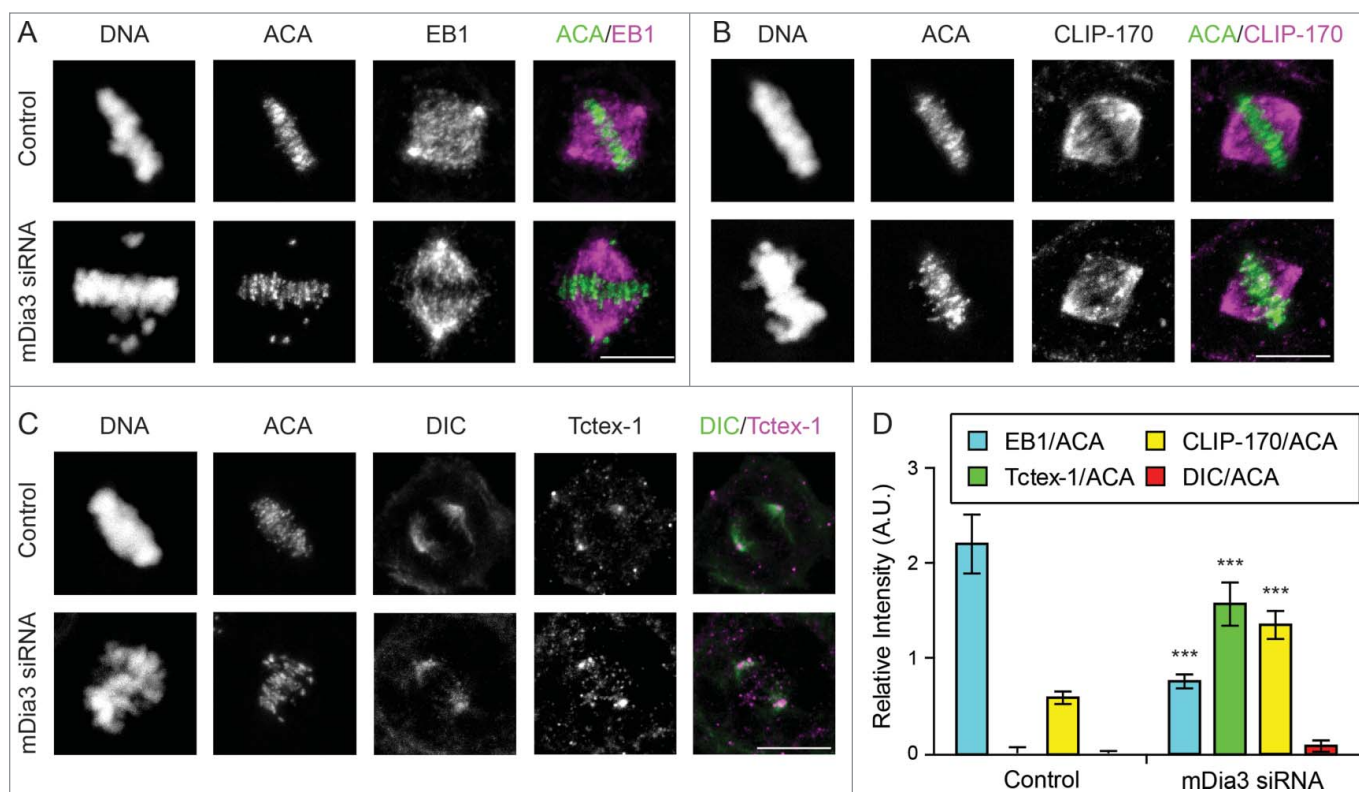


Figure 1. CLIP-170 and Tctex-1, but not dynein, remain at attached kinetochores without mDia3 and EB1. (A–C) Indirect immunofluorescence staining of DNA (DAPI staining) and ACA, along with EB1 (A), CLIP-170 (B), Dynein (DIC in C), and Tctex-1 (C) in control and mDia3 knockdown metaphase cells as indicated (72 hr post-transfection). Cells were treated with nocodazole for 4 hrs and then released into MG132 for 1 hr prior to fixation. Bar, 5 μ m. (D) Quantification of the relative intensities (per kinetochore) at aligned kinetochores of EB1/ACA, CLIP-170/ACA, DIC/ACA, and Tctex-1/ACA in metaphase cells (mean with 95% confidence interval, $P < 0.0001$ as indicated by *** based on more than 30 kinetochores from at least 5 cells).

not affect the release of cytoplasmic dynein from aligned kinetochores, judging by the loss of kinetochore staining of dynein intermediate chain (DIC) (Fig. 1C and D). In contrast, the level of Tctex-1, a dynein light chain, is significantly increased on aligned kinetochores in mDia3 knockdown cells (Fig. 1C and D). These results show that at least a population of Tctex-1 and CLIP-170 can be recruited onto kinetochores without dynein.

Tctex-1 is an outer kinetochore component

To confirm that Tctex-1 is a kinetochore component, we examined the kinetochore localization of Tctex-1 in fixed cells (Fig. 2A). Indirect immunofluorescence showed strong Tctex-1 kinetochore staining, which colocalized with ACA, during mitosis but not interphase. Tctex-1 associated with kinetochores in prophase and remained at the kinetochore until metaphase. Furthermore, in late prometaphase cells, we detected Tctex-1 kinetochore signals on unaligned, but not aligned, chromosomes. Using N-SIM super-resolution microscopy system, we examined the localization of Tctex-1 within the kinetochore and found that Tctex-1 localized peripherally to Hec1, a component of the outer kinetochore protein complex Ndc80 (Fig. 2B). In addition, in cells treated with monastrol to produce monopolar spindles with monotelic chromosomes (with only one sister

kinetochore attached to microtubule and the other unattached), Tctex-1 localized to only one of 2 sister kinetochores on many chromosomes (Fig. S1A). The strong Tctex-1 staining was observed on the kinetochore further from the pole while the kinetochore closer to the pole had much less Tctex-1 staining. This asymmetric staining of sister kinetochores on monotelic chromosomes in monastrol-treated cells are similar to previously documented kinetochore localization of Mad2, a mitotic checkpoint protein which localizes only to unattached kinetochores.²² These results collectively suggest that Tctex-1 is an outer kinetochore component and associates only with unattached kinetochores.

Cytoplasmic dynein is also recruited onto unattached kinetochores and departs from attached kinetochores along with mitotic checkpoint proteins through a dynein self-removal mechanism.²³ Despite the similar kinetochore localization pattern, we identified some differences in the timing in which Tctex-1 appeared at kinetochores in comparison with dynein. Judging by immunofluorescence staining compared to late prometaphase kinetochores, the prophase and early prometaphase kinetochores were able to recruit a significant amount of Tctex-1 with no or little dynein (Fig. S1B). This result is consistent with the possibility that the recruitment of Tctex-1 onto unattached kinetochores can occur independently of dynein.

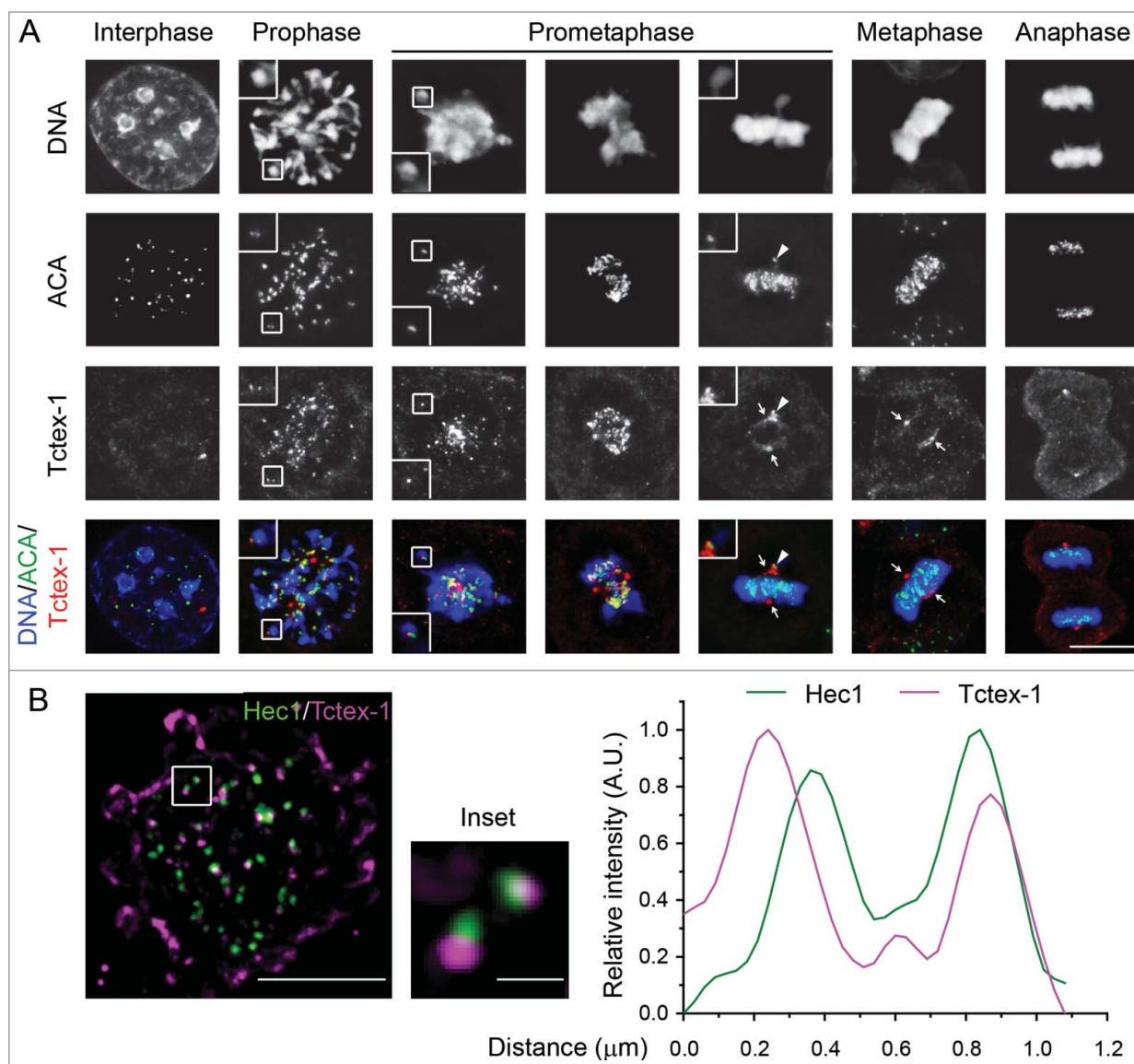


Figure 2. The dynein light chain Tctex-1 associates with unattached kinetochores. **(A)** Immunofluorescence detection of ACA, Tctex-1, and DNA (DAPI staining) in mitotic cells. In merged panels: ACA – green, Tctex-1 – red, and DNA – blue. Insets: colocalization of Tctex-1 and ACA at a pair of sister kinetochores. Arrows point to spindle poles and arrow heads point to unattached kinetochores on a polar chromosome. Bar, 5 μm. **(B)** Left panel: N-SIM Super-resolution images showing Hec1 (green) and Tctex-1 (magenta). Right panel: graph showing a representative linescan of the fluorescent intensity of a pair of sister kinetochores that is highlighted in left panel (inset).

Tctex-1 plays a role in metaphase chromosome alignment and accurate chromosome segregation, and this function is independent of its ability to bind to dynein

To test for the functions of Tctex-1 at the kinetochore, we transfected cells with a plasmid encoding Tctex-1 short hairpin RNA (shRNA) and far red fluorescent protein (HcRed). The expression of Tctex-1 shRNA had resulted in a clear reduction of Tctex-1 protein level after either 48 hr (Fig. 3A), as well as 72 hr (data not shown), and a loss of Tctex-1 at unattached kinetochores by immunofluorescence microscopy (Fig. 3B). The loss of Tctex-1 at kinetochores could be rescued by expressing a shRNA-resistant Flag-tagged

Tctex-1 construct (Fig. 3B), further supporting that Tctex-1 is a kinetochore component.

Chromosome movement and mitotic progression upon Tctex-1 depletion were assessed by live cell imaging in unperturbed mitoses using cells stably expressing the Histone H2B-EYFP fusion protein. Depletion of Tctex-1 (72 hr post-transfection of the Tctex-1 shRNA construct) extended the average duration of mitosis (to 171 min) compared to control cells (51 min) (Figs. 3C and 4D, Movies S1 and S2). More importantly, this mitotic delay is caused by a few chromosomes chronically misaligned near the spindle poles, which were subsequently missegregated at anaphase onset (Figs. 3D, 4E and F). The existence of

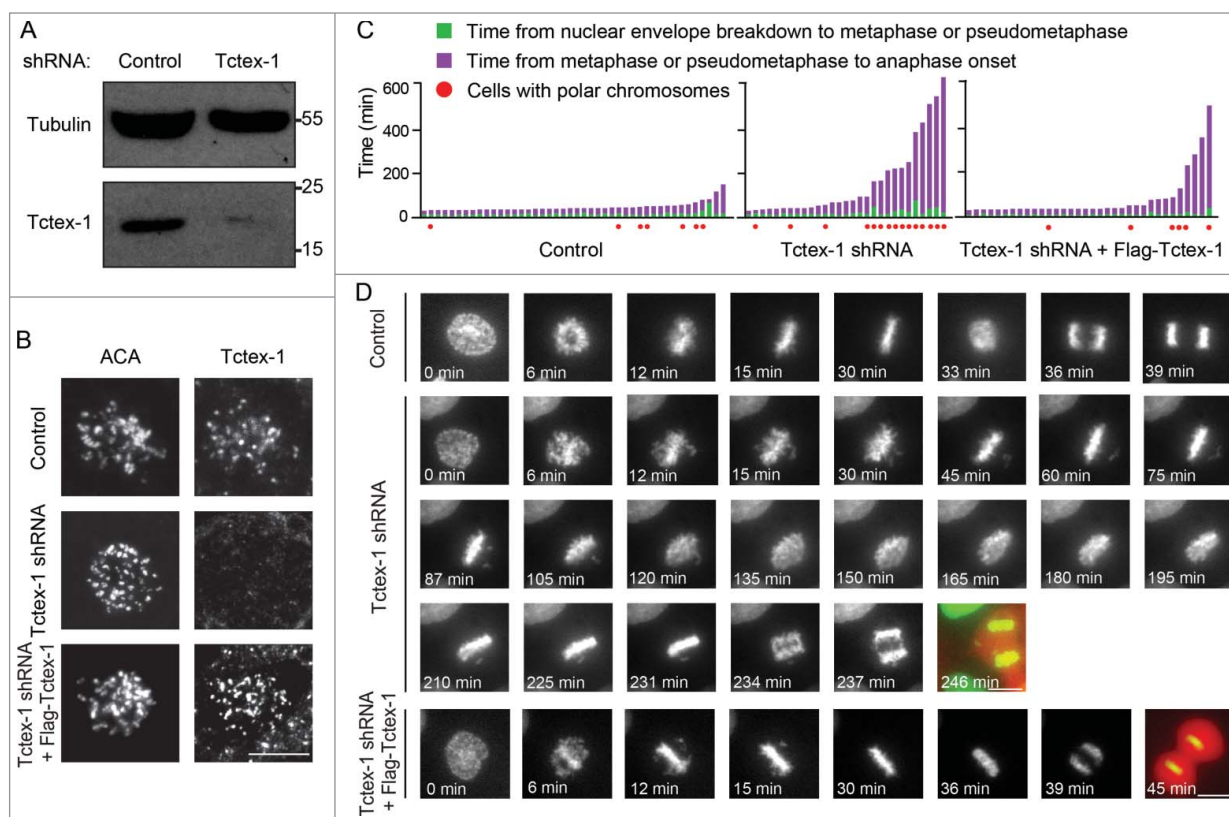


Figure 3. Tctex-1 is essential for accurate chromosome segregation. **(A)** Immunoblotting of cell lysates 48 hr posttransfection with control or Tctex-1 shRNA plasmids as indicated. **(B)** Immunofluorescence staining of ACA and Tctex-1 in mitotic cells 48 hr posttransfected with control or Tctex-1 shRNA plasmids, as well as the wild-type Flag-Tctex-1 expression vector, as indicated. For Tctex-1 shRNA + Flag-Tctex-1 cells, Tctex-1 was stained with anti-Flag antibody. Bar, 5 μ m. **(C)** Time spent from nuclear envelope breakdown to metaphase (or pseudometaphase) (green) and from metaphase (or pseudometaphase) to anaphase onset (magenta) of cells (expressing H2B-EYFP) transiently transfected with control or Tctex-1 shRNA plasmids, as well as the wild-type Flag-Tctex-1 vector (72 hr post-transfection). Each vertical bar represents a single cell. The transfected cells were identified by HcRed, which are coexpressed by the shRNA plasmid, before live cell imaging. Pseudometaphase is designated as when the majority of chromosomes are aligned with an obvious metaphase plate and a few polar chromosomes. **(D)** Stills of live-cell imaging showing cells transfected with control or Tctex-1 shRNA plasmids, as well as the wild-type Flag-Tctex-1 expression vector, as indicated, during unperturbed mitoses. The transfected cell was identified by cytosolic red signals from the co-expression of HcRed as showed in the last still image. Bar, 5 μ m.

only a few unaligned chromosomes is consistent with the observation that Tctex-1 depletion did not affect the overall cold-stable microtubules in metaphase cells (Fig. S2). Besides polar chromosomes, many Tctex-1-depleted cells also exhibited chromosome bridges upon anaphase onset. The importance of Tctex-1 in mitotic progression is confirmed by the rescue with the expression of the shRNA resistant wild-type Flag-Tctex-1 protein in Tctex-1-depleted cells (Figs. 3B–D). These results demonstrate that Tctex-1 is important for metaphase chromosome alignment and accurate chromosome segregation.

Tctex-1 directly binds to dynein intermediate chain and has a predicted threonine 94 (T94) phosphorylation site.¹⁹ Only the nonphosphorylatable Tctex-1-T94A protein, but not the phosphomimetic Tctex-1-T94E protein, is able to associate with the dynein complex.¹⁹ In agreement, we confirmed that both Flag-wild type Tctex-1 and Flag-Tctex-1-T94A, but not Flag-Tctex-1-T94E, were co-immunoprecipitated with endogenous dynein (DIC) in mitotic extracts (Fig. 4A). We examined whether the expression of these 2 Tctex-1 proteins can rescue mitotic defects

caused by the depletion of endogenous Tctex-1. Judging by live cell imaging, both Tctex-1-T94A and Tctex-1-T94E substantially reduced the duration of mitosis to a similar degree (Figs. 4B–D, Movies S3 and S4). Furthermore, the incidents of misaligned and missegregated chromosomes were similarly reduced in cell expressing T94A and T94E for the rescue (Fig. 4B, C and F). These results confirm an important role of Tctex-1 for accurate chromosome segregation and suggest that this function of Tctex-1 at the kinetochore does not depend on its interaction with dynein.

Tctex-1 knockdown does not affect dynein-Tctex-1L at kinetochores

It has been shown that another dynein light chain DYNLT3/Tctex-1L associates with kinetochores and binds to Bub3, a mitotic checkpoint protein.²⁴ These results have been interpreted as the Tctex-1L to contribute to dynein cargo binding specificity. We examined whether the chromosome misalignment and missegregation phenotype caused by

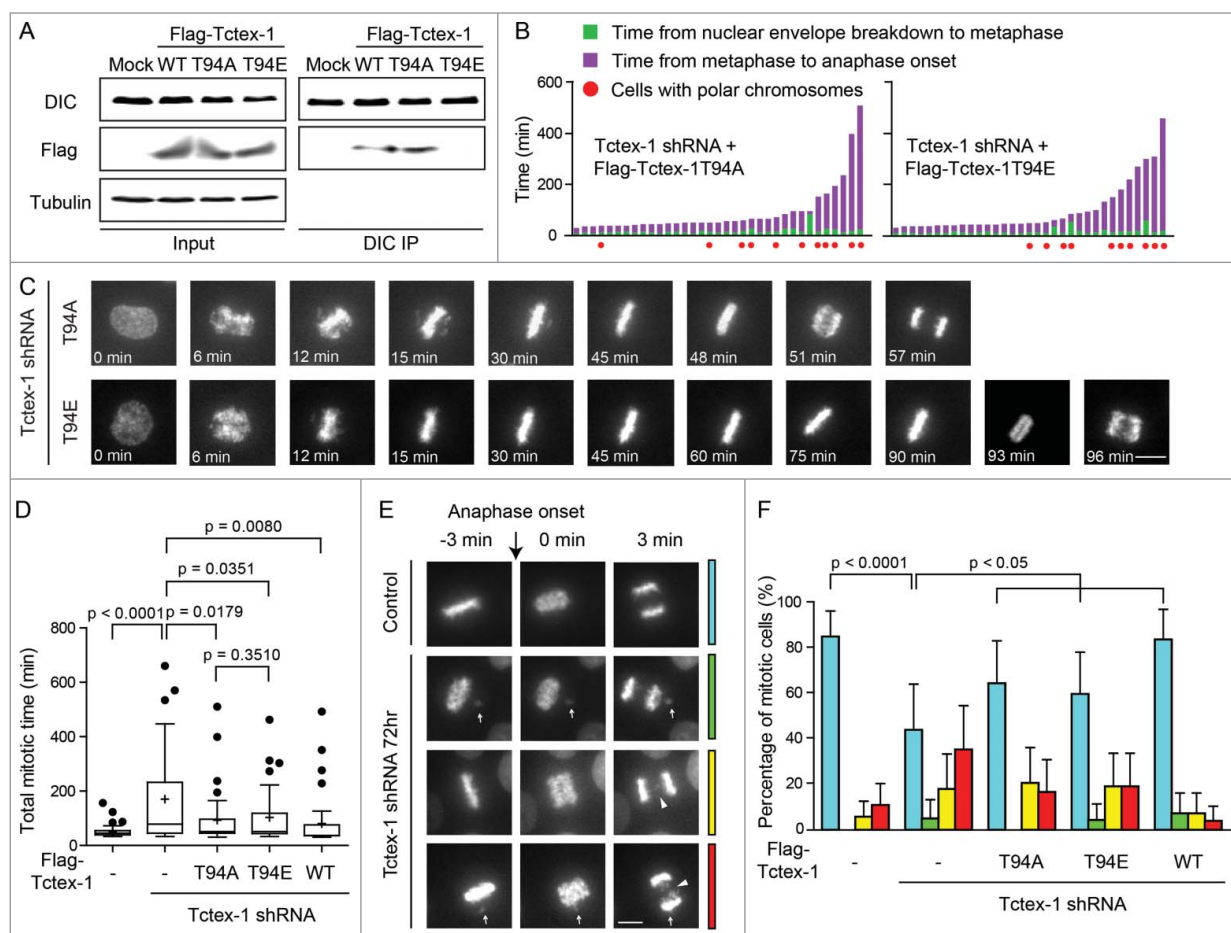


Figure 4. The mitotic role of Tctex-1 does not depend on its interaction with dynein. **(A)** Immunoprecipitates from mitotic cell extracts with DIC antibody and then probed with DIC and Flag antibodies as indicated. Cells were transfected with Flag tagged wild-type Tctex-1, Tctex-1T94A or Tctex-1-T94E. **(B)** Time spent from nuclear envelope breakdown to metaphase (or pseudometaphase) (green) and from metaphase (or pseudometaphase) to anaphase onset (magenta) of cells (expressing H2B-EYFP) transiently transfected with Tctex-1 shRNA plasmids and expression vectors for the nonphosphorylatable Tctex-1T94A or the phosphomimetic Tctex-1T94E variants (72 hr post-transfection). Each vertical bar represents a single cell. **(C)** Stills of live-cell imaging showing cells transfected with Tctex-1 shRNA plasmids and expression vectors for the nonphosphorylatable Tctex-1T94A or the phosphomimetic Tctex-1T94E variants, as indicated, during unperturbed mitoses. Bar, 5 μ m. **(D)** Distribution of total time spent in mitosis (from nuclear envelope breakdown to anaphase onset) in cells transfected with shRNAs and expression vectors as indicated. Whisker-Tukey boxes span 25-75 percentile, while center bar denotes median and "+" marks mean. **(E)** Stills of live-cell imaging showing a control cell and cells transfected with Tctex-1 shRNA plasmids at the anaphase onset. Arrows indicate missegregated polar chromosomes and arrow heads indicate chromosome bridges. Bar, 5 μ m. **(F)** The percentage of mitotic cells with normal segregation (blue), missegregated polar chromosomes (green), chromosome bridges (yellow), and both (red) at the anaphase onset were analyzed in cells transfected with shRNAs and expression vectors as indicated. Mean with 95% confidence interval were plotted with chi-square test used to compute the p-value.

Tctex-1 depletion could attribute to the change of the population of dynein-Tctex-1L at kinetochores. Indirect immunofluorescence analysis revealed that Tctex-1L indeed associated with unattached kinetochores along with dynein (DIC) (Fig. S3A and B) as reported previously.²⁴ Depletion of ZW10 from unattached kinetochores resulted in a significant loss of both dynein (DIC) and Tctex-1L to a similar extent (Fig. S3A and B), suggesting that the kinetochore association of Tctex-1L is dependent of dynein. In contrast, depletion of Tctex-1 did not change the amount of Tctex-1L associated with unattached kinetochores (Fig. S3C and D). These results clearly suggest that depletion of Tctex-1 does not affect the pool of dynein-Tctex-1L at kinetochores.

The kinetochore localization of Tctex-1 is independent of cytoplasmic dynein

An important role for dynein during mitosis is to transport of mitotic checkpoint proteins off kinetochores toward spindle poles upon microtubule capture.²³ BubR1 and Mad1 are 2 mitotic checkpoint proteins whose kinetochore localization depends on microtubule attachment.^{25,26} Immunofluorescence staining revealed the presence of BubR1 and Mad1 at unattached kinetochores of polar chromosomes, but not on attached kinetochores of chromosomes aligned at the metaphase plate in both control and Tctex-1 depleted cells (Fig. 5). This suggests that depletion of the dynein light chain Tctex-1 does not have an effect on dynein-dependent removal of mitotic checkpoint

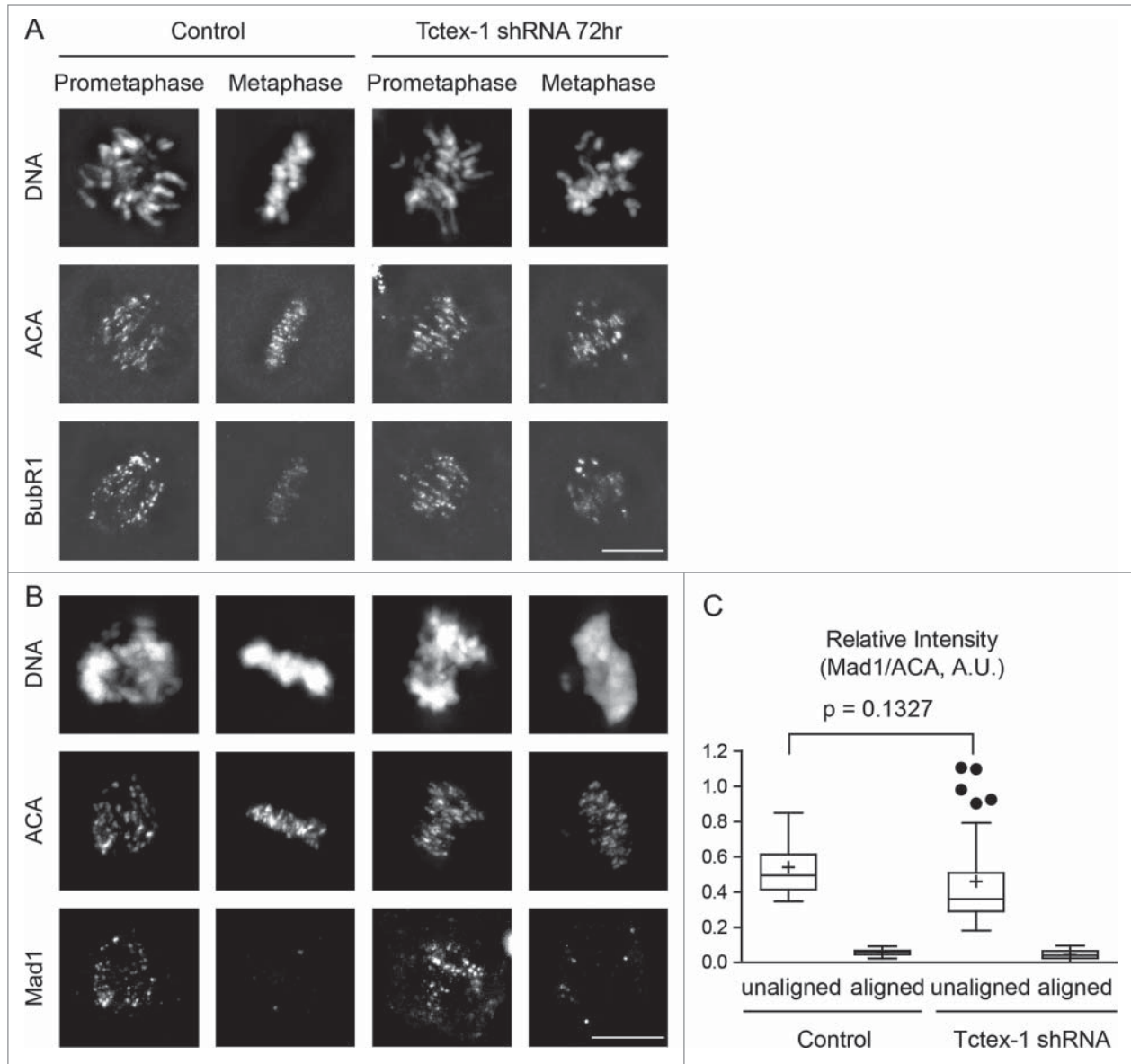


Figure 5. Tctex-1 depletion does not affect the association of the mitotic checkpoint proteins at unattached kinetochores and their release from attached kinetochores. **(A and B)** Immunofluorescence detection of DNA, ACA, BubR1 **(A)** and Mad1 **(B)** in prometaphase and metaphase cells transfected with control or Tctex-1 shRNA plasmids as indicated. Bar, 5 μ m. **(C)** Quantification of the normalized relative kinetochores intensities (per kinetochores) of Mad1/ACA in mitotic cells. Whisker-Tukey boxplots span 25–75 percentile, while center bar denotes median and “+” marks mean. Quantifications were based on 30 kinetochores (control unaligned), 30 kinetochores (control aligned), 37 kinetochores (Tctex-1 shRNA unaligned) and 30 kinetochores (Tctex-1 shRNA aligned) from multiple cells.

proteins from attached kinetochores. Furthermore, this result supports the idea that Tctex-1 has a direct role on microtubule capture at unattached kinetochores independent of dynein.

To further test a possible dynein-independent role of Tctex-1 at the kinetochores, we examined the inter-dependency of kinetochores recruitment between Tctex-1 and cytoplasmic dynein. Depletion of Tctex-1 from unattached kinetochores did not affect kinetochores association of cytoplasmic dynein **(Fig. 6A and B)**. Furthermore, knocking down of ZW10, a component of the RZZ (Rod/ZW10/

Zwilch) complex that recruits dynein to kinetochores,^{27,28} significantly reduced the level of dynein at unattached kinetochores **(Fig. 6A and C)**. By contrast, ZW10 suppression only modestly diminished kinetochores recruitment of Tctex-1 **(Fig. 6A and C)**. In combination with the observation of Tctex-1 localization at kinetochores without dynein in mDia3 knockdown cells **(Fig. 1C and D)** and prophase cells **(Fig. S1B)**, these results demonstrate that at least a portion of Tctex-1 can be recruited onto unattached kinetochores independent of dynein.

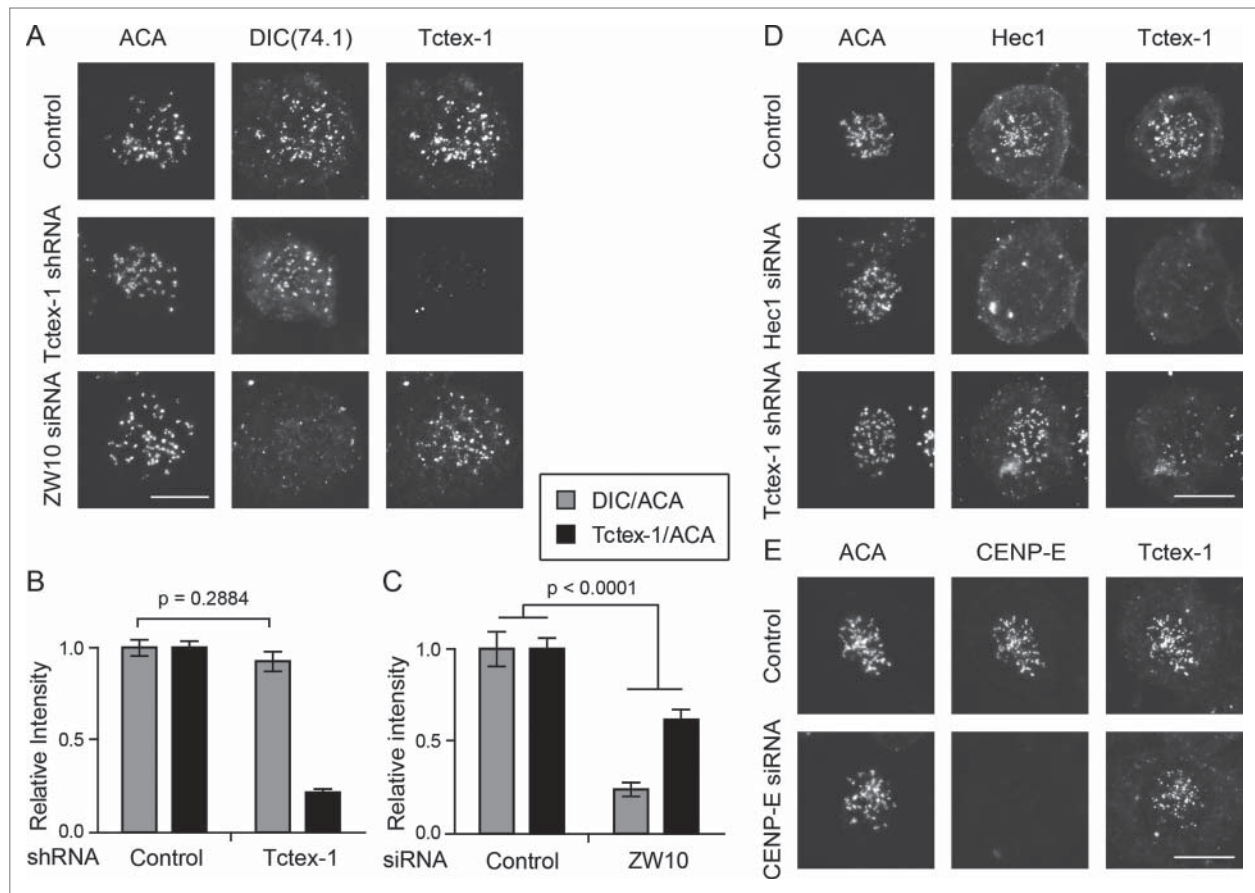


Figure 6. Tctex-1 kinetochore localization is dynein independent. **(A)** Immunofluorescence detection of ACA, dynein (DIC), and Tctex-1 in nocodazole treated (3 hrs) mitotic cells transfected with Tctex-1 shRNA plasmids or ZW10 siRNA as indicated. Bar, 5 μ m. **(B and C)** Quantification of the normalized relative kinetochore intensities (per kinetochore) of DIC/ACA and Tctex-1/ACA (mean \pm SEM) in mitotic cells. In **(B)**, 63 (control) and 57 (Tctex-1 shRNA) kinetochores from multiple cells were measured. In **(C)**, 83 (control) and 41 (ZW10 siRNA) kinetochores from multiple cells were measured. **(D and E)** Immunofluorescence detection of ACA, Hec1 **(A)** or CENP-E **(B)**, and Tctex-1 in mitotic cells transfected with Hec1 **(A)** or CENP-E **(B)** siRNA. Bar, 5 μ m.

Tctex-1 kinetochore localization depends on the Ndc80 complex

The position of Tctex-1 in the hierarchical structure of the kinetochore will clearly provide us with crucial indications of Tctex-1's role at the kinetochore. To understand how Tctex-1 is targeted to the kinetochore, we searched for kinetochore components that are required for kinetochore recruitment of Tctex-1. We found that the level of Tctex-1 on unattached kinetochores was substantially reduced in Hec1 (a component of the Ndc80 complex) knockdown cells (Fig. 6D, middle panel), suggesting an Ndc80-dependent kinetochore localization of the Tctex-1 protein. Conversely, knockdown of Tctex-1 did not affect kinetochore recruitment of the Ndc80 complex (Hec1) (Fig. 6D, bottom panel). Furthermore, depletion of CENP-E, the microtubule plus end-directed motor, did not affect the recruitment of Tctex-1 onto unattached kinetochores (Fig. 6E). Depletion of Ndc80 components does not significantly affect the level of dynein at kinetochores.²⁹ Thus, this result is consistent with a dynein-independent recruitment of Tctex-1 onto kinetochores.

Discussion

It has been suggested that both Dynein-dynactin complex and CLIP-170 are present only at the unattached kinetochores and are released upon microtubule attachment.³⁰ The kinetochore localization of CLIP-170 might depend on the dynein/dynactin pathway.³¹⁻³⁴ We now show that CLIP-170 and Tctex-1, but not cytoplasmic dynein, remains at attached kinetochores which lack EB1 upon depletion of the formin mDia3. Our work argues that the dissociation of CLIP-170 from attached kinetochores is neither a direct response from microtubule attachment nor through a dynein-dependent removal pathway. Instead, the removal of CLIP-170 might involve changes of microtubule plus-end dynamics regulated by the accumulation of EB1 through its interaction with the kinetochore-associated mDia3 protein. Furthermore, this result also indicates that the kinetochore localization of Tctex-1, a dynein light chain, does not depend on the dynein complex.

Increasing evidence suggests that dynein light chains can bind to proteins other than cytoplasmic dynein in diverse cellular

functions.¹⁸ Our study unravels an important function for the dynein light chain Tctex-1 at the kinetochore in a dynein independent manner. Evidence for this model includes the following. First, Tctex-1 can be recruited onto kinetochores through dynein-independent mechanisms. Tctex-1 associates with dynein-free kinetochores in prophase cells and in ZW10 knock-down cells, suggesting that at least part of Tctex-1 enriched at unattached kinetochores is free from the dynein complex. Second, depletion of Tctex-1 does not affect dynein self-removal and the removal of the mitotic checkpoint proteins from attached kinetochores, implying that Tctex-1 is not functionally important for kinetochore-associated dynein. Third, a phosphomimetic Tctex-1T94E protein, which has been shown to be unable to incorporate into the dynein complex in transfected cells¹⁹ and now by coimmunoprecipitation analysis using mitotic cell extracts, can rescue mitotic defects caused by the depletion of endogenous Tctex-1 proteins just like its nonphosphorylatable counterpart Tctex-1T94A that can associate with the dynein complex. And fourth, depletion of the Ndc80 complex, but not ZW10-dynein, at unattached kinetochores results in a significant loss of Tctex-1. These results coherently suggest that the functional role in metaphase chromosome alignment and accurate chromosome segregation by kinetochore-associated Tctex-1 is largely independent from its association with the dynein complex.

Induction of a dimeric Tctex-1 “trap” results in rapidly disruption of early endosomal and lysosomal organization, but has no obvious effect on mitosis.³⁵ On one hand, these results support that Tctex-1 is not functionally important for dynein in mitotic progression. On the other hand, these results, along with other observations, indicate that kinetochore-associated Tctex-1 proteins may be not in rapid exchange with the free cytosolic pool, as is observed with dynein for endosomes and lysosomes. Structural studies support a role for dynein light chains to promote protein dimerization and structural stabilization.¹⁸ These light chains can allosterically bind to and regulate, besides dynein, diverse proteins and protein complexes. Future work will require the identification of the binding partner for the dynein-independent population at kinetochores.

Materials and Methods

Cell culture, transfection, and drug treatment

T98G cells were maintained in DME medium supplemented with 10% FBS at 37°C in 5% CO₂. The Tctex-1 shRNA construct and rescue plasmids are as described previously.^{19,20} Transfection was performed using HiPerfect (QIAGEN) based on the manufacturer’s instructions (48 hr or 72 hr, as indicated in figures/figure legends), and cells transfected with shRNA were identified by the co-expressed HcRed. The mDia3 siRNA was purchased from QIAGEN. ZW10 and CLIP-170 siRNAs were purchased from Dharmacon (Thermo Scientific) and used as instructed by the manufactures. Nocodazole, monastrol and MG132 were purchased from Sigma-Aldrich and used at final concentrations of 100 ng/ml, 100 μM and 10 μM, respectively.

All drug treatments were performed for particular length of time, as described in figure legends.

Immunofluorescence microscopy and live cell imaging

A commercial Tctex-1 antibody (H-60, Santa Cruz) was used in this study for all the data obtained. ACA (purified human anti-centromere protein IgG) was from Antibodies Inc. Other commercial antibodies used in this study included anti-EB1 (1A11/4 & H-70, Santa Cruz), anti-CLIP-170 (F3 & H300, Santa Cruz), anti-Flag-M2 (F3165, Sigma-Aldrich), anti-DIC (74.1, Ab23905, Abcam), anti-Hec1 (9G3, Abcam), anti-αTubulin(DM1α, T6199, Sigma-Aldrich), anti-BubR1(8G1, Abcam), anti-Mad1 (9B10, Santa Cruz), anti-CENP-E (C-5, Santa Cruz), and anti-Tctex-1L (E15, Santa Cruz).

For indirect immunofluorescence, cells grown on poly-D-lysine coated coverslips were washed in pre-warmed PBS, extracted with 0.1% Triton-X-100 in PBS for 1 min, fixed in cold methanol at –20°C for 10 min, and blocked in 5% BSA in PBS at 4°C overnight. Coverslips were subjected to primary antibodies diluted in PBS and DyLight488, Rhodamine or Cy5 conjugated secondary antibodies (Jackson Immuno-Research Laboratories, Inc.), both at room temperature for 1 hr. DAPI (final concentration 16.67 ng/mL) was used to stain nuclei/chromosomes. Coverslips were mounted using antifade reagent (ProLong Gold; Molecular Probes). Images were acquired at room temperature using an inverted microscope (IX81; Olympus) with a 60×, NA 1.42 Plan Apochromat oil immersion objective (Olympus), a monochrome charge-coupled device camera (Sensicam QE; Cooke Corporation), which are controlled by the SlideBook software (3i and Olympus). 10 z-sections 0.5 μm apart spanning 5 μm were taken for each cell. All images in each experiment along with appropriate controls were collected on the same day with identical exposure time. No-neighbor deconvolution and/or maximum z-projection was performed on selected stacks of representative images, which were subsequently scaled in ImageJ (NIH) or MATLAB (Mathworks, Inc.) for visual comparison. Quantitative image analysis was performed with ImageJ (NIH). To measure fluorescent intensities at each individual kinetochore, unassigned unit 16-bit tiff images of whole stacks or of maximum z-projections were exported from the SlideBook with all bit depth information being preserved. ROIs (regions of interest) were generated covering each kinetochore based on channel-merged image and the integrated pixel intensities were then measured for each channel within the ROI. In each cell, 5 cytosolic ROIs near the kinetochore ROIs were also quantitated as above and averaged for background subtraction. Intensity data were then subjected to ratio calculation and normalization before plotting.

For live cell imaging, cells stably expressing H2B-EYFP were plated onto Poly-D-Lysine coated 35 mm glass-bottom dishes (MatTek Corporation) and maintained in CO₂ independent medium (Gibco #18045) supplemented with 4 mM L-glutamine and 10% FBS, with an environmentally controlled chamber at 37°C during imaging. Images were acquired every 3 min using an inverted microscope (IX81; Olympus) with a 40×, NA 0.6 LUCPLFLN air objective (Olympus) and a interline transfer cooled CCD camera (ORCA-R2 C10600-10B; HAMAMATSU

Photonics), which were controlled by the MetaMorph software (Molecular Devices, LLC).

Structured Illumination Microscopy (N-SIM)

Cells grown on No. 1.5 (0.17 mm thick) cover glasses coated with poly-D-lysine were washed, extracted and fixed as in common immunofluorescence. Endogenous Ndc80 and Tctex-1 proteins were recognized by mouse anti-hec1 antibody (9G3, Abcam) and rabbit anti-Tctex-1 (H-60, Santa Cruz), which were subsequently labeled by secondary antibodies conjugated with DyLight488 (Jackson Immuno-Research Laboratories, Inc.) and Alexa Fluor 568 (Life Technologies), respectively. ProLong Gold without DAPI (Life Technologies) was used as mounting medium to achieve a refractive index as close to 1.515 as possible. Mounted samples were completely cured and sealed before imaging. To rule out any potential shift between different channels due to the optics of the microscope, a custom-built reference slide was used for channel alignment and post-hoc pixel registration. Manufacturer's imaging procedure (N-SIM, Nikon) was followed. In particular, a 100x oil objective (Apo TIRF 100x Oil DIC N2, NA 1.49) was used in conjunction with Andor DU-897 X-6050 EMCCD camera. 3D-SIM mode imaging was performed with laser lines 488 and 561 nm at constant temperature under control. 41 z-sections 0.125 μm apart spanning 5 μm were taken with MCL NanoDrive PiezoZ Drive. For each z-section, 15 different moiré fringes resulted from illuminations with known, high spatial frequency patterns were captured. Reconstruction was performed with N-SIM module inside NIS-Elements using optimal parameters, to create super-resolution images by processing multiple moiré patterns.

Immunoprecipitation and immunoblotting analysis

Immunoprecipitation were performed using Dynabeads[®] following standard protocol provided by the manufacturer (Life technologies) with minor modifications. Confluent mitotic cells (arrested in nocodazole for 9 hrs) growing on 10 cm dish were trypsinized and collected into 50 ml vials. Centrifugations were performed (with second time in PBS supplemented with protease inhibitor cocktail, Roche 04-693-159-001) at 4°C, 1500 rpm for 5 min each to harvest cells. Dynabeads with Protein G (Life technologies) were washed in PBS for 3 times, and incubated with primary antibodies (anti-dynein intermediate chain 74.1) at a ratio of 10 μg antibodies per 1 mg beads, for 2 hrs on 4°C rocker. IP lysis buffer [1% NP-40, 25 mM Tris-HCl (pH 7.5), 150 mM NaCl, 5 mM EDTA (pH 8.0)] supplemented with protease inhibitor cocktail was added into the harvested cells (400 μl per sample), mixed well and incubated on 4°C rocker for 30 min, after which DNA were destroyed with syringe needle (BD-25G5/8) followed by additional 15 min incubation. The lysate mixture was then centrifuged at 12000 rpm for 10 min to remove insoluble materials, after which 20 μl input was retrieved, boiled with SDS sample buffer and stored. After incubation with primary antibodies,

beads were washed 3 times. 380 μL of the supernatant of cell lysate were then added into the beads and gently homogenized by pipetting. Beads-lysate mixture were incubated on 4°C rocker for 1 hr, after which the beads were washed 3 times and boiled in SDS sample buffer [30% glycerol, 350 mM 1M Tris (pH 6.8), 10% SDS, 0.05% bromophenol blue and 5% 2-mercaptoethanol].

For immunoblotting, cells were lysed in RIPA buffer [50 mM Tris-HCl (pH 7.5), 150 mM NaCl, 1% NP-40, 0.1% SDS, 0.5% Na-Deoxycholate Acid] and denatured in SDS sample buffer. Cell lysates were then subjected to 10% SDS-PAGE followed by membrane transfer (Immobilon-P, Millipore; Towbin transfer buffer, pH 8.3). Immunoblots on the membrane were blocked with Tris-buffered saline with tween (TBST) [20 mM Tris-HCl (pH 7.4), 150 mM NaCl, 0.05% Tween] containing nonfat dry milk and then probed with affinity-purified primary antibodies in TBST. Primary antibodies were visualized using horseradish peroxidase (HRP)-labeled goat secondary antibodies and enhanced chemiluminescence (ECL), or using AF680 anti mouse (Life technologies) and IRDye800 anti rabbit antibodies (LI-COR Biosciences) together with the LI-COR imaging system (LI-COR Biosciences).

Statistical analysis and graphing

All statistical analyses were done in Prism 5 (Graphpad) or Stata 12 (StataCorp, LP). Unpaired two-tailed student's t-test was performed at the 5% level of significance unless otherwise noted. Statistical decisions are made after computing p-values: $p > 0.05$, not significant; p is between 0.01 and 0.05, significant; p is between 0.001 and 0.01, very significant; $P < 0.001$, extremely significant. Two-way ANOVA test was performed in particular experiments to test if the interaction between 2 variables [e.g. treatment (control/siZW10) *v.s.* protein (DIC/Tctex-1) in Fig. 6C and Fig. S3B] is significant at the 5% level of significance. After calculation, a significant outcome suggests that the effects of treatment (siZW10) vary by different proteins (i.e. DIC and Tctex-1 behave significantly differently upon the same treatments). All graphs were prepared in either Prism 5 (Graphpad) or Origin 8.6 (OriginLab).

Disclosure of Potential Conflicts of Interest

No potential conflicts of interest were disclosed.

Acknowledgments

We thank all members of the Mao laboratory for stimulating discussion. We also thank Ruijun Zhu (Columbia University), Lynne Chang (Nikon) and the Marine Biological Laboratory for technical helps with the Structured Illumination Microscopy.

Funding

This work has been supported by grants from the National Institute of Health (GM89768 to Y.M. and EY11307 to C.-H.

S.) and research awards from the Irma T. Hirsch/Monique Weill-Caulier Trusts (Y.M.) and Research to Prevent Blindness (C.-H.S.).

Supplemental Material

Supplemental data for this article can be accessed on the publisher's website.

References

- Cheerambathur DK, Desai A. Linked in: formation and regulation of microtubule attachments during chromosome segregation. *Curr Opin Cell Biol* 2014; 26:113-22; PMID:24529253; <http://dx.doi.org/10.1016/j.ccb.2013.12.005>
- Guo Y, Kim C, Mao Y. New insights into the mechanism for chromosome alignment in metaphase. *International review of cell and molecular biology* 2013; 303:237-62; PMID:23445812; <http://dx.doi.org/10.1016/B978-0-12-407697-6.00006-4>
- Cleveland DW, Mao Y, Sullivan KF. Centromeres and kinetochores: from epigenetics to mitotic checkpoint signaling. *Cell* 2003; 112:407-21; PMID:12600307; [http://dx.doi.org/10.1016/S0092-8674\(03\)00115-6](http://dx.doi.org/10.1016/S0092-8674(03)00115-6)
- De Rop V, Padeganeh A, Maddox PS. CENP-A: the key player behind centromere identity, propagation, and kinetochore assembly. *Chromosoma* 2012; 121:527-38; PMID:23095988; <http://dx.doi.org/10.1007/s00412-012-0386-5>
- Rago F, Cheeseman IM. Review series: the functions and consequences of force at kinetochores. *J Cell Biol* 2013; 200:557-65; PMID:23460675; <http://dx.doi.org/10.1083/jcb.201211113>
- Varma D, Salmon ED. The KMN protein network—chief conductors of the kinetochore orchestra. *J Cell Sci* 2012; 125:5927-36; PMID:23418356; <http://dx.doi.org/10.1242/jcs.093724>
- Daum JR, Wren JD, Daniel JJ, Sivakumar S, McAvoy JN, Potapova TA, Gorbsky GJ. Ska3 is required for spindle checkpoint silencing and the maintenance of chromosome cohesion in mitosis. *Curr Biol* 2009; 19:1467-72; PMID:19646878; <http://dx.doi.org/10.1016/j.cub.2009.07.017>
- Gaitanos TN, Santamaria A, Jeyaprakash AA, Wang B, Conti E, Nigg EA. Stable kinetochore-microtubule interactions depend on the Ska complex and its new component Ska3/C13Orf3. *Embo Journal* 2009; 28:1442-52; PMID:19360002; <http://dx.doi.org/10.1038/emboj.2009.96>
- Raaijmakers JA, Tanenbaum ME, Maia AF, Medema RH. RAMA1 is a novel kinetochore protein involved in kinetochore-microtubule attachment. *J Cell Sci* 2009; 122:2436-45; PMID:19549680; <http://dx.doi.org/10.1242/jcs.051912>
- Welburn JP, Grishchuk EL, Backer CB, Wilson-Kubalek EM, Yates JR, 3rd, Cheeseman IM. The human kinetochore Ska1 complex facilitates microtubule depolymerization-coupled motility. *Dev Cell* 2009; 16:374-85; PMID:19289083; <http://dx.doi.org/10.1016/j.devcel.2009.01.011>
- Cheng L, Zhang J, Ahmad S, Rozier L, Yu H, Deng H, Mao Y. Aurora B regulates formin mDia3 in achieving metaphase chromosome alignment. *Developmental Cell* 2011; 20:342-52; PMID:21397845; <http://dx.doi.org/10.1016/j.devcel.2011.01.008>
- Yasuda S, Ocegüera-Yanez F, Kato T, Okamoto M, Yonemura S, Terada Y, Ishizaki T, Narumiya S. Cdc42 and mDia3 regulate microtubule attachment to kinetochores. *Nature* 2004; 428:767-71; PMID:15085137; <http://dx.doi.org/10.1038/nature02452>
- Mao Y, Varma D, Vallee R. Emerging functions of force-producing kinetochore motors. *Cell Cycle* 2010; 9:715-9; PMID:20160491; <http://dx.doi.org/10.4161/cc.9.4.10763>
- Mao Y. FORMIN a link between kinetochores and microtubule ends. *Trends in cell biology* 2011; 21:625-9; PMID:21920754; <http://dx.doi.org/10.1016/j.tcb.2011.08.005>
- Tamura N, Draviam VM. Microtubule plus-ends within a mitotic cell are 'moving platforms' with anchoring, signalling and force-coupling roles. *Open biology* 2012; 2:120132; PMID:23226599; <http://dx.doi.org/10.1098/rsob.120132>
- Tynan SH, Gee MA, Vallee RB. Distinct but overlapping sites within the cytoplasmic dynein heavy chain for dimerization and for intermediate chain and light intermediate chain binding. *J Biol Chem* 2000; 275:32769-74; PMID:10893223; <http://dx.doi.org/10.1074/jbc.M001537200>
- Tai AW, Chuang JZ, Bode C, Wolfrum U, Sung CH. Rhodopsin's carboxy-terminal cytoplasmic tail acts as a membrane receptor for cytoplasmic dynein by binding to the dynein light chain Tctex-1. *Cell* 1999; 97:877-87; PMID:10399916; [http://dx.doi.org/10.1016/S0092-8674\(00\)80800-4](http://dx.doi.org/10.1016/S0092-8674(00)80800-4)
- Rapali P, Szemes A, Radnai L, Bakos A, Pal G, Nyitrai L. DYNLL/LC8: a light chain subunit of the dynein motor complex and beyond. *The FEBS journal* 2011; 278:2980-96; PMID:21777386; <http://dx.doi.org/10.1111/j.1742-4658.2011.08254.x>
- Chuang JZ, Yeh TY, Bollati F, Conde C, Canavosio F, Caceres A, Sung CH. The dynein light chain Tctex-1 has a dynein-independent role in actin remodeling during neurite outgrowth. *Dev Cell* 2005; 9:75-86; PMID:15992542; <http://dx.doi.org/10.1016/j.devcel.2005.04.003>
- Li A, Saito M, Chuang JZ, Tseng YY, Dedesma C, Tomizawa K, Kaitsuka T, Sung CH. Ciliary transition zone activation of phosphorylated Tctex-1 controls ciliary resorption, S-phase entry and fate of neural progenitors. *Nat Cell Biol* 2011; 13:402-11; PMID:21394082; <http://dx.doi.org/10.1038/ncb2218>
- Yeh C, Li A, Chuang JZ, Saito M, Caceres A, Sung CH. IGF-1 activates a cilium-localized noncanonical gbetagamma signaling pathway that regulates cell-cycle progression. *Dev Cell* 2013; 26:358-68; PMID:23954591; <http://dx.doi.org/10.1016/j.devcel.2013.07.014>
- Kapoor TM, Mayer TU, Coughlin ML, Mitchison TJ. Probing spindle assembly mechanisms with monastrol, a small molecule inhibitor of the mitotic kinesin, Eg5. *J Cell Biol* 2000; 150:975-88; PMID:10973989; <http://dx.doi.org/10.1083/jcb.150.5.975>
- Howell BJ, McEwen BF, Canman JC, Hoffman DB, Farrar EM, Rieder CL, Salmon ED. Cytoplasmic dynein/dynactin drives kinetochore protein transport to the spindle poles and has a role in mitotic spindle checkpoint inactivation. *J Cell Biol* 2001; 155:1159-72; PMID:11756470; <http://dx.doi.org/10.1083/jcb.200105093>
- Lo KW, Kogoy JM, Pfister KK. The DYNLT3 light chain directly links cytoplasmic dynein to a spindle checkpoint protein, Bub3. *J Biol Chem* 2007; 282:11205-12; PMID:17289665; <http://dx.doi.org/10.1074/jbc.M611279200>
- Guo Y, Kim C, Ahmad S, Zhang J, Mao Y. CENP-E-dependent BubR1 autophosphorylation enhances chromosome alignment and the mitotic checkpoint. *J Cell Biol* 2012; 198:205-17; PMID:22801780; <http://dx.doi.org/10.1083/jcb.201202152>
- Rozier L, Guo Y, Peterson S, Sato M, Baer R, Gautier J, Mao Y. The MRN-CtIP Pathway Is Required for Metaphase Chromosome Alignment. *Mol Cell* 2013; PMID:23434370
- Starr DA, Williams BC, Hays TS, Goldberg ML. ZW10 helps recruit dynactin and dynein to the kinetochore. *J Cell Biol* 1998; 142:763-74; PMID:9700164; <http://dx.doi.org/10.1083/jcb.142.3.763>
- Whyte J, Bader JR, Tauhata SB, Raycroft M, Hornick J, Pfister KK, Lane WS, Chan GK, Hinchcliffe EH, Vaughan PS, et al. Phosphorylation regulates targeting of cytoplasmic dynein to kinetochores during mitosis. *J Cell Biol* 2008; 183:819-34; PMID:19029334; <http://dx.doi.org/10.1083/jcb.200804114>
- DeLuca JG, Moree B, Hickey JM, Kilmartin JV, Salmon ED. hNuf2 inhibition blocks stable kinetochore-microtubule attachment and induces mitotic cell death in HeLa cells. *J Cell Biol* 2002; 159:549-55; PMID:12438418; <http://dx.doi.org/10.1083/jcb.200208159>
- Maiato H, Fairley EA, Rieder CL, Swedlow JR, Sunkel CE, Earnshaw WC. Human CLASP1 is an outer kinetochore component that regulates spindle microtubule dynamics. *Cell* 2003; 113:891-904; PMID:12837247; [http://dx.doi.org/10.1016/S0092-8674\(03\)00465-3](http://dx.doi.org/10.1016/S0092-8674(03)00465-3)
- Coquelle FM, Caspi M, Cordelieres FP, Dompierre JP, Dujardin DL, Koifman C, Martin P, Hoogenraad CC, Akhmanova A, Galjart N, et al. LIS1, CLIP-170's key to the dynein/dynactin pathway. *Mol Cell Biol* 2002; 22:3089-102; PMID:11940666; <http://dx.doi.org/10.1128/MCB.22.9.3089-3102.2002>
- Dujardin D, Wacker UI, Moreau A, Schroer TA, Rickard JE, De Mey JR. Evidence for a role of CLIP-170 in the establishment of metaphase chromosome alignment. *J Cell Biol* 1998; 141:849-62; PMID:9585405; <http://dx.doi.org/10.1083/jcb.141.4.849>
- Liang Y, Yu W, Li Y, Yu L, Zhang Q, Wang F, Yang Z, Du J, Huang Q, Yao X, et al. Nudel modulates kinetochore association and function of cytoplasmic dynein in M phase. *Mol Biol Cell* 2007; 18:2656-66; PMID:17494871; <http://dx.doi.org/10.1091/mbc.E06-04-0345>
- Tai CY, Dujardin DL, Faulkner NE, Vallee RB. Role of dynein, dynactin, and CLIP-170 interactions in LIS1 kinetochore function. *J Cell Biol* 2002; 156:959-68; PMID:11889140; <http://dx.doi.org/10.1083/jcb.200109046>
- Varma D, Dawn A, Ghosh-Roy A, Weil SJ, Ori-McKenney KM, Zhao Y, Keen J, Vallee RB, Williams JC. Development and application of in vivo molecular traps reveals that dynein light chain occupancy differentially affects dynein-mediated processes. *Proc Natl Acad Sci U S A* 2010; 107:3493-8; PMID:20133681; <http://dx.doi.org/10.1073/pnas.0908959107>